THE JOURNAL OF PHYSICAL CHEMISTRY B

Article

pubs.acs.org/JPCB

Molecular Dynamics Simulations of the Interactions of DMSO with DPPC and DOPC Phospholipid Membranes

Zak E. Hughes,[†] Alan E. Mark,[§] and Ricardo L. Mancera*[,†,‡]

[†]Western Australian Biomedical Research Institute, Curtin Health Innovation Research Institute, School of Biomedical Sciences, and [‡]School of Pharmacy, Curtin University, P.O. Box U1987, Perth, WA 6845, Australia

[§]School of Chemistry and Molecular Biosciences and Institute for Molecular Bioscience, The University of Queensland, Brisbane, QLD 4072, Australia

Supporting Information

ABSTRACT: Molecular dynamics simulations have been used to investigate the effect of DMSO on 1,2-dipalmitoyl-*sn*-glycero-3-phosphatidylcholine (DPPC) and 1,2-dioleoyl-*sn*-glycero-3-phosphocholine (DOPC) phospholipid bilayers. The concentration of DMSO was varied between 0 and 25.0 mol %. For both lipids, DMSO causes the membrane to expand in the plane of the membrane while thinning normal to that plane. Above a critical concentration, pores in the membrane form spontaneously, and if the concentration is increased further, then the bilayer structure is destroyed. Even at concentrations below those required to induce pores, DMSO readily diffuses across the bilayers. The free-energy profile associated with the diffusion of a DMSO molecules across the membrane has been calculated. The simulations suggest that the DOPC bilayer is more resistant to the deleterious effects of DMSO, both increasing the stability of the membranes and decreasing the rate at which DMSO diffuses across the membrane. In this way, the work highlights the importance of investigating the lipid composition of cell membranes when characterizing the effects of cryosolvents.

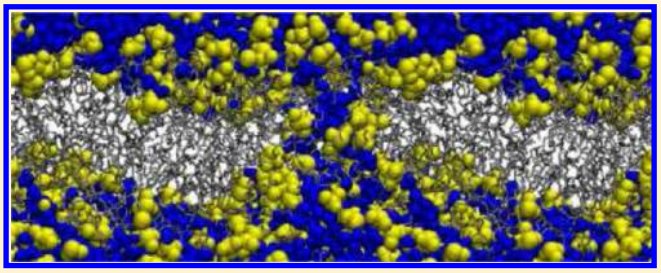

INTRODUCTION

A wide variety of biological tissues are required to be stored for years or even decades, posing a considerable challenge. One way of storing biological material is through cryopreservation,[1−6] where the sample is stored at liquid nitrogen temperatures (77 K), ensuring that any biological, chemical, and physical processes occurring at either the intra- or extra-cellular level are halted. This allows viable samples to be stored for decades without any change in their structure. In addition, cryopreservation often offers advantages to traditional storage methods in terms of space and cost, as samples need only minor care once they have been successfully cryopreserved. To help to reduce the damage to cells that can occur during the cryopreservation process, biological samples are often treated with an aqueous solution containing a number of different cryoprotective agents (CPAs).[7−9]

One of the most widely used CPAs is dimethylsulfoxide (DMSO).[8−10] DMSO can penetrate through the cell membrane[11] and promote the vitrification of water upon rapid cooling, avoiding the deleterious formation of intracellular ice. The presence of DMSO and other CPAs broadens the glass transition of water, which has been suggested to be the basis for the strengthening of the glassy state of water and the reduction in the likelihood of crystallization.[12,13] Although widely used as a CPA, DMSO can be toxic to cells even at low concentration, making it preferable to use the lowest possible DMSO concentration that will prevent ice formation.[14] DMSO has also been shown to have anti-inflammatory[15] and anesthetic properties[16] and can induce cell fusion.[17] For all of these reasons, it is important to understand how DMSO interacts with cells at the molecular level.

There have been a number of studies investigating the effects of DMSO on membranes, both experimentally[11,18−23] and computationally.[24−27] Experimental studies, using X-ray diffraction and differential scanning calorimetry (DSC),[18,22] suggest that in aqueous solution DMSO interacts strongly with the headgroup region of the lipid bilayer. An increase in the area per lipid (APL) and thinning of the membrane have also been observed. The results of infrared spectroscopy indicate that DMSO dehydrates phospholipid membranes[20,23] and increases the gel−liquid-crystalline phase-transition temperature.[21] In water, the liquid-crystal−gel phase transition temperature of 1,2-dipalmitoyl-*sn*-glycero-3-phosphatidylcholine (DPPC) is 314.4 K,[28] whereas in a solution of 10 mol % DMSO the transition temperature is increased to 320 K.[20] This shift in the transition temperature increases as the concentration of the solution increases such that in pure DMSO the gel phase is stable up to 350 K.[20]

Previous molecular dynamics (MD) simulation studies of the effect of DMSO on phospholipid membranes have yielded results in qualitative agreement with experiment.[24−27,30−32]

Received: April 12, 2012
Revised: September 3, 2012
Published: September 4, 2012

dx.doi.org/10.1021/jp3035538 | *J. Phys. Chem. B* 2012, 116, 11911−11923

In the presence of DMSO, DPPC membranes expand laterally while thinning normal to the plane of the membrane. At DMSO concentrations of 7−20 mol %, pores are observed to form in the bilayer. At higher concentrations, the structure of the bilayer is destroyed. The formation of pores in DPPC membranes has been observed in both atomistic[27,30,31] and coarse-grained simulations.[29] In addition to DPPC membranes, the effect of DMSO on 2-oleoyl-1-palmitoyl-*sn*-glycero-3-phosphocholine (POPC) and 1,2-dimyristoyl-*sn*-glycero-3-phosphocholine (DMPC) membranes has been studied.[31,33,34] The effect of DMSO on POPC and DMPC bilayers is qualitatively the same as that on DPPC, with lateral expansion of the bilayer and pore formation observed. The formation of a pore within the bilayer structure encouraged phospholipids to "flip" between the two leaflets of the membrane.[31] The number of "flips" increased with temperature and decreased as the length of the phospholipid tails increased. The pores formed in the bilayers have been shown to reduce the energy barrier associated with the diffusion of salt ions across the membrane.[30]

Plant and animal membranes, however, contain a diverse range of lipid species, and to understand truly how DMSO interacts with biological membranes, we must quantify its interaction with different phospholipid species. For example, a recent study evaluating the type and amount of phospholipid species present in plant cells[35] found that the majority of phosphocholine lipids present in three plant species had 18 carbon acyl tails. Moreover, the degree of unsaturation of the lipids was significant in all three species. Therefore, in an initial attempt to better represent plant membranes, 1,2-dioleoyl-*sn*-glycero-3- phosphocholine (DOPC) has been chosen as a model system in this work. The longer acyl chains present in DOPC compared with DPPC means that the bilayer is thicker;[36,37] however, because the acyl chains of DOPC have a carbon−carbon double bond at C9, DOPC bilayers are less ordered than DPPC bilayers. The liquid-crystal−gel phase transition of DOPC in water is 255.7 K,[38] which is significantly lower than that of DPPC (314.4 K).[28] The aim of this work was thus to determine if changes in the acyl chains of the phospholipid alter the effect of DMSO on the membrane by comparing the results of simulations of DPPC and DOPC systems.

METHODS

The recently developed GROMOS 53A6$_L$ force field[36,37] was used to model the phospholipids. These parameters, which form part of the GROMOS 54A7 force field,[39] reproduce a broad range of membrane properties. The water molecules were represented by the SPC model,[40] and the DMSO molecules were represented by a rigid united-atom model that forms part of the standard GROMOS 53A6 and 54A7 force fields.[39,41]

The simulations were performed using GROMACS v.3.3.3.[42] Twin-range cutoffs were used for the nonbonded interactions: interactions within 0.8 nm were calculated every step, and interactions within 1.4 nm were updated every five timesteps along with the pair list. A reaction-field correction was applied using a relative dielectric permittivity constant, ε_{RF} = 62, suitable for SPC water, to account for the truncation of electrostatic interactions beyond the 1.4 nm cutoff.[40] Simulations of lipid bilayer systems comparing the reaction-field method against Ewald sum methods[25,43,44] have determined that there are no significant differences between the two approaches. The equations of motion were integrated using the leapfrog algorithm with a time step of 2 fs.[45] The simulations were performed in the NpT ensemble, with the box

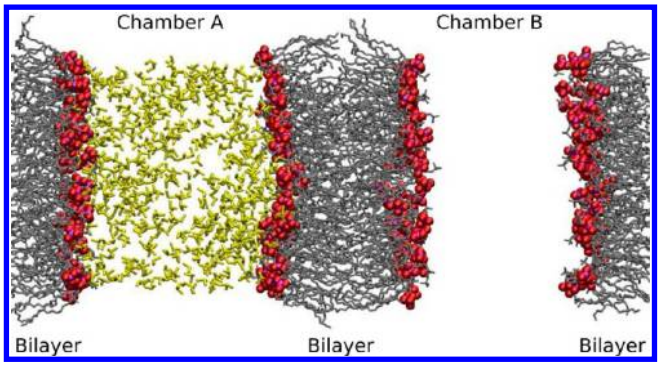

Figure 1. Snapshot of a double-bilayer system illustrating the initial system configuration. The phosphorus headgroups are represented by the spheres. The phospholipids and DMSO molecules are colored gray and yellow, respectively. The water molecules are not shown for clarity.

Table 1. Area Per Lipid (APL) and Membrane Thickness, D_{HH}, of DPPC and DOPC Phospholipid Bilayers at Different Concentrations of DMSO at a Temperature of 350 K, Determined from Simulation

lipid	[DMSO]/mol %	APL/nm^2	D_{HH}/nm
DPPC	0	0.654 ± 0.010	3.02
	1.25	0.688 ± 0.011	2.91
	2.50	0.721 ± 0.011	2.81
	5.00	0.769 ± 0.017	2.56
	10.0	0.859 ± 0.014	2.21
	12.5		1.46
	15.0		
	20.0		
	25.0		
DOPC	0	0.683 ± 0.008	3.11
	1.25	0.720 ± 0.012	3.06
	2.50	0.747 ± 0.015	2.94
	5.00	0.805 ± 0.015	2.61
	10.0	0.874 ± 0.019	2.39
	12.5	0.903 ± 0.018	2.21
	15.0		1.41
	20.0		0.89
	25.0		

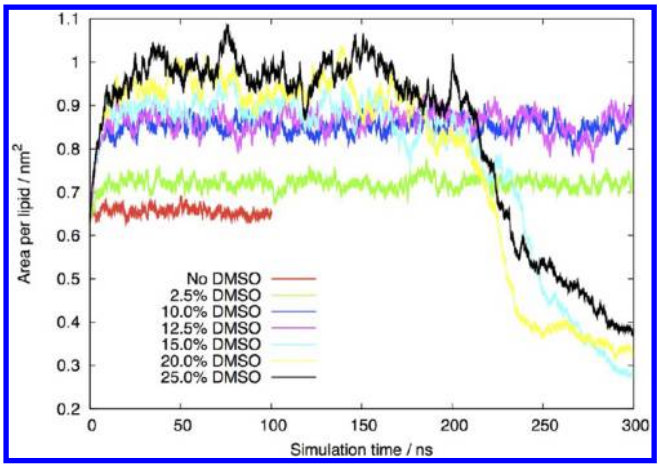

Figure 2. Evolution of the area per lipid (APL) with time of the DPPC membranes at a different DMSO concentrations and 350 K.

dx.doi.org/10.1021/jp3035538 | J. Phys. Chem. B 2012, 116, 11911−11923

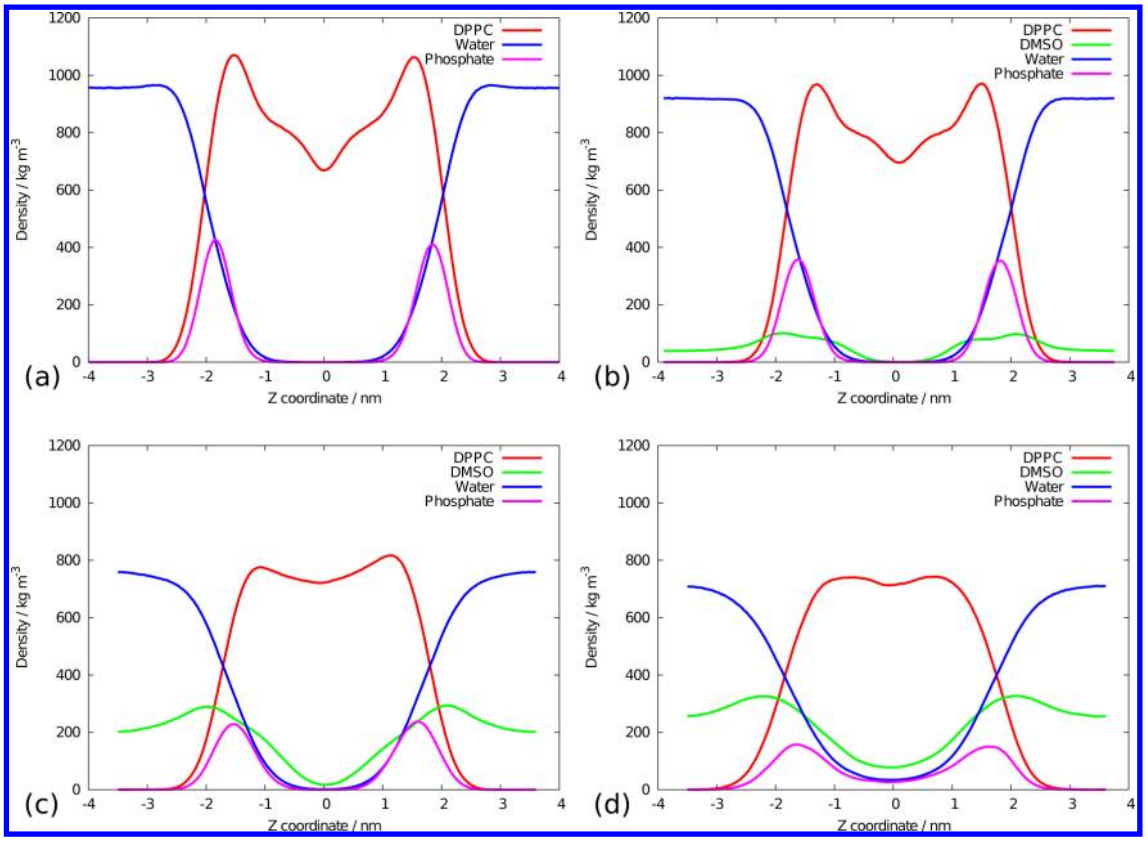

Figure 3. Density profiles perpendicular to the plane of the membrane of DPPC membranes in solutions of (a) 0, (b) 2.5, (c) 10.0, and (d) 12.5 mol % DMSO.

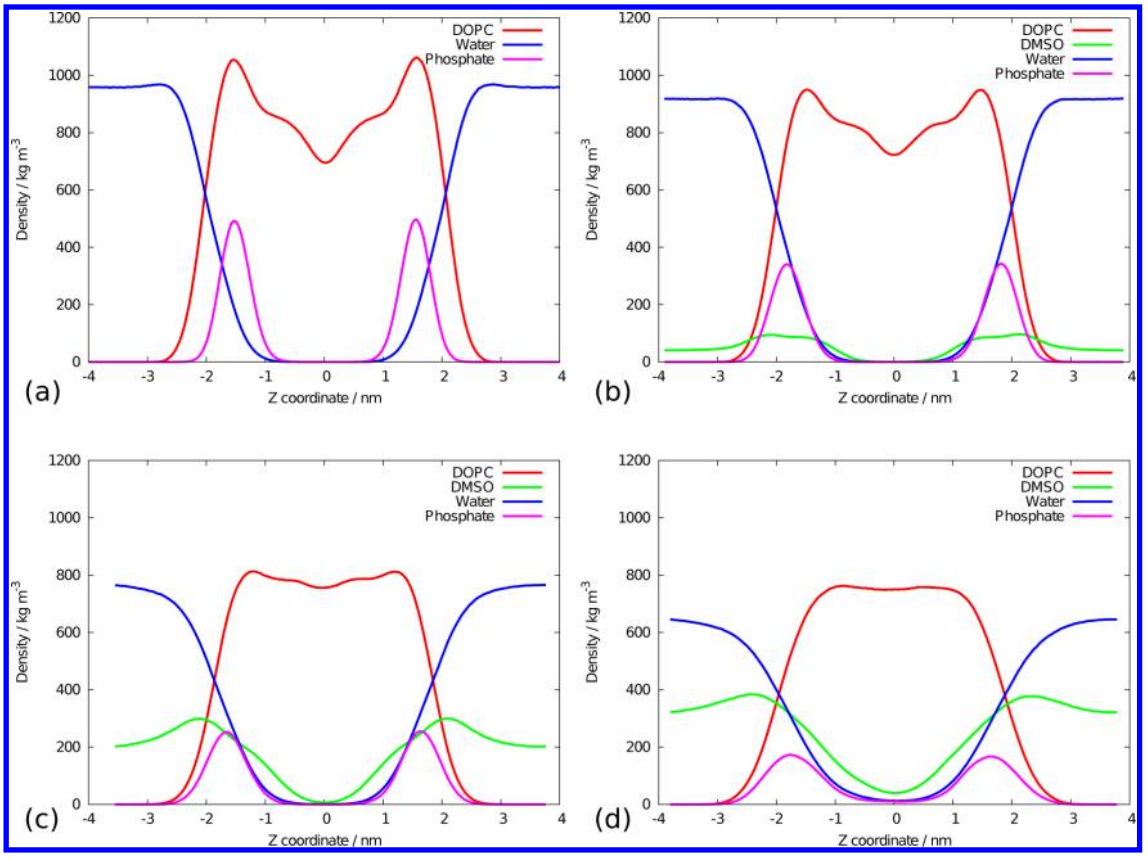

Figure 4. Density profiles perpendicular to the plane of the membrane of DOPC membranes in solutions of (a) 0, (b) 2.5, (c) 10.0, and (d) 15.0 mol % DMSO.

dx.doi.org/10.1021/jp3035538 | J. Phys. Chem. B 2012, 116, 11911−11923

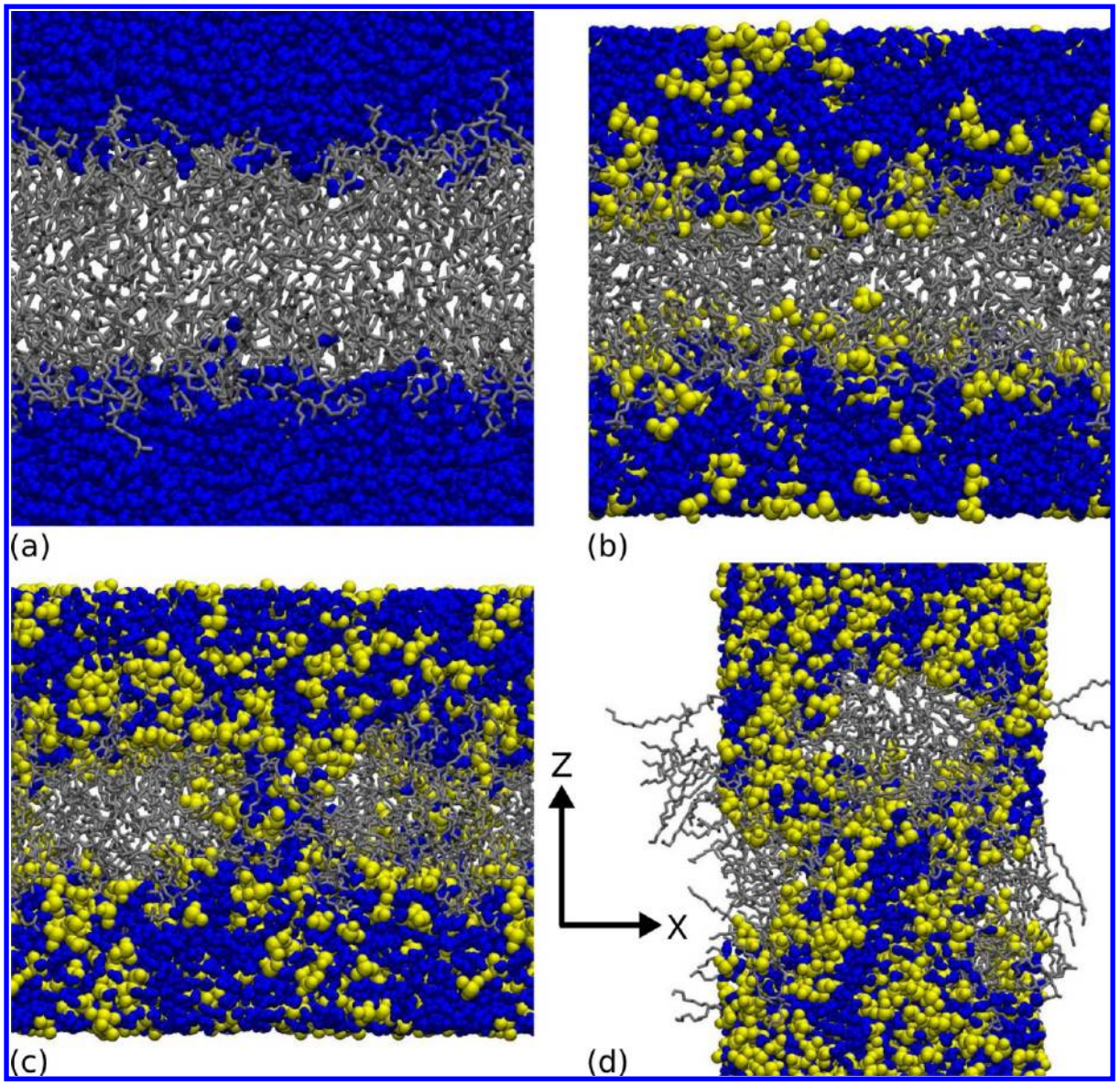

Figure 5. Snapshots taken from simulations of a DOPC membrane in (a) 0, (b) 10.0, (c) 15.0, and (d) 25.0 mol % DMSO. The phospholipids, water, and DMSO molecules are colored gray, blue, and yellow, respectively.

dimensions parallel and perpendicular to the plane of the bilayer independently coupled to a pressure bath at 1 bar.[46] The isothermal compressibility was set to 4.6×10^{-5} bar^{-1}, and the coupling constant, τ_P, was set to 1 ps. The temperature of the systems was kept constant by independently coupling the lipids and solvent molecules to an external temperature bath with a coupling constant of 0.1 ps using a Berendsen thermostat.[46]

DMSO is known to promote the formation of a gel phase.[20,21] As a consequence, most previous simulations have been performed at a temperature of 350 K to ensure that the system was in the liquid-crystal phase. The simulations here were performed at a temperature of 350 K to allow comparison with previous work. The initial configurations of the membranes were taken from pre-equilibrated DPPC and DOPC membranes solvated in water at temperatures of 323 and 303 K, respectively.[47] The bilayers, consisting of a total of 128 lipids, were gradually heated over 20 ns to 350 K before being allowed to equilibrate at this temperature for 100 ns. The total number of solvent molecules was fixed at 5841, corresponding to ~46 solvent molecules per lipid. Both lipids were simulated in solutions of 0, 1.25 2.50, 5.00, 10.0, 12.5, 15.0, 20.0, and 25.0 mol % DMSO, where the DMSO mole percent (mol %) of the solution is equal to the mole fraction of DMSO multiplied by 100. Typically, when cryopreserving plant species, 10 wt % (~2.5 mol %) solutions are used. The simulations were performed at higher concentrations to (1) determine the upper limit that lipid bilayers are able to tolerate and (2) ensure the DMSO interacted rapidly with the membrane given the fact that the simulations were limited to a nanosecond time scale. For the DPPC systems with DMSO concentrations of 2.5, 15.0, and 25.0 mol %, further simulations with 8762 solvent molecules were performed to ensure that the membrane was not interacting with itself. Because the results (not shown) of these simulations proved to be within statistical error of the systems with 5841 solvent molecules, the DOPC systems were simulated only with the smaller number of solvent molecules. Unless otherwise stated, each system containing DMSO was simulated for 300 ns with the last 60 ns of simulation time being used for analysis.

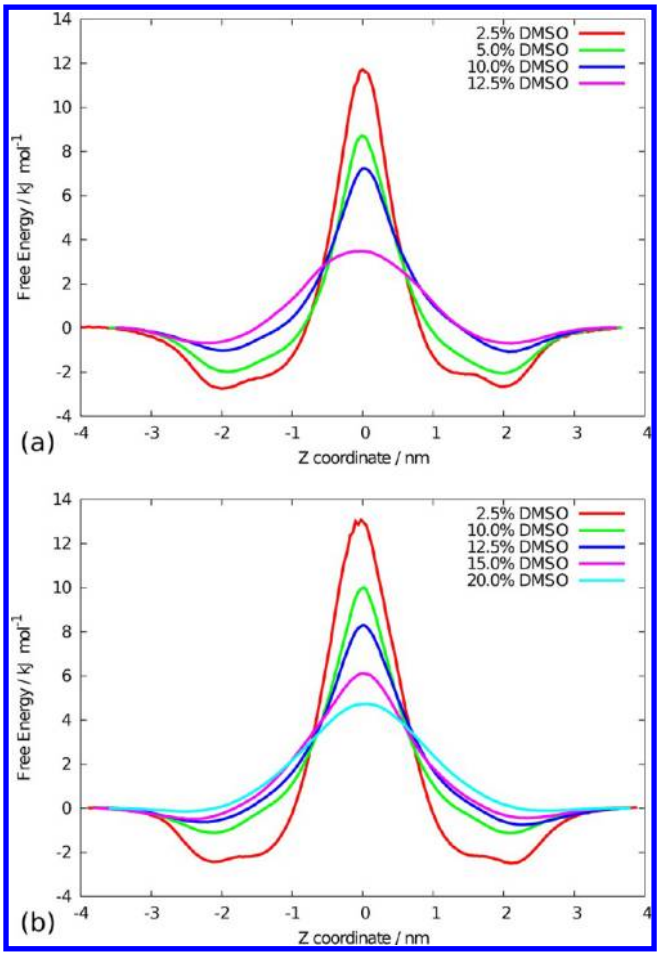

Figure 6. Free-energy profiles for the diffusion of a DMSO molecule across (a) a DPPC membrane bilayer and (b) a DOPC membrane at different DMSO concentrations.

In addition to simulations of a single-bilayer, a number of simulations were performed on systems consisting of two bilayers using the setup that was previously used by Leekumjorn and Sum.[26] This enabled a concentration gradient to be established, initially, across the bilayer. This was achieved by having one solvent layer (chamber A) initially consisting solely of water molecules, whereas the other contained a solution of water and DMSO (chamber B). The total number of solvent molecules in each layer was initially 5841. Both the DPPC and DOPC membranes were simulated in solutions with a total DMSO concentration (i.e., across both chambers) of 1.25 and 5.00 mol %. A snapshot showing the initial configuration of one double-bilayer system is shown in Figure 1. These simulations were also performed at a temperature of 350 K and a pressure of 1 atm.

RESULTS AND DISCUSSION

Single-Bilayer Systems. After an initial overview of the results of the simulations is given, a comparison between the results obtained in this study and those of previous works will be presented. This will then be followed by a discussion of the differences between the effect of DMSO on the DPPC and DOPC systems.

The effect of DMSO on APL and the thickness of the membrane for the different systems is summarized in Table 1. The APL of DPPC in water was determined to be 0.654 nm^2. This is lower than the experimental value of 0.719 nm^2 but falls within the range of APLs (0.650 to 0.690 nm^2) that previous simulations of DPPC in water at 350 K have given.[25−27,48] The presence of DMSO causes an increase in the APL of the both the DPPC and DOPC membranes, indicating that the membrane expands laterally upon the addition of DMSO. Plots of the APL as a function of simulation time are shown in Figure 2. As can be seen in Figure 1, the APL increases rapidly during the first 20−40 ns of the simulation before stabilizing. Below concentrations of 15.0 and 25.0 mol % for DPPC and DOPC, respectively, the expanded membranes are stable, at least on the 300 ns time scales simulated. However, at or above these concentrations the bilayer structure is only metastable and undergoes a sudden and catastrophic collapse, as indicated by the rapid drop in APL. The time between the initial expansion of the membrane and its ultimate collapse was on the order of hundreds of nanoseconds, highlighting the need to simulate the systems for extended periods of time. The relative increase in the APL of the DPPC and DOPC membranes is approximately the same. The APL of DOPC is ∼4% larger than that of DPPC at a DMSO concentration of 5.0 mol % or less. The difference in the APL of the two lipid species is reduced slightly (2%) at 10.0 mol %, but this is most likely within the uncertainty of the calculations.

The lateral expansion of the membrane is accompanied by a concurrent decrease in the thickness of the membrane normal to the plane of the bilayer, D_{HH} (calculated as the distance between the two peaks in the lipid density profile). The degree of thinning is approximately linear with respect to the DMSO concentration until a threshold concentration is reached, at which point the values of D_{HH} drop significantly. This drop in the D_{HH} occurs at a concentration lower than that at which the membrane becomes unstable, 12.5 mol % for DPPC and 15.0 mol % for DOPC.

The density profiles of the systems normal to the plane of the bilayer over the last 60 ns of the simulations are shown in Figures 3 and 4. Snapshots of the corresponding systems for the DOPC membrane are shown in Figure 5. From Figures 3 and 4 it can be seen that at low DMSO concentrations (2.5 mol %) DMSO molecules accumulate at the surface of the membrane in the headgroup region with few molecules penetrating beyond the phosphate groups. Nevertheless, there is a clear loss of structure compared with that in the absence of DMSO, even in the center of the bilayer, as indicated by the flatter profile. As the concentration of DMSO is increased the effects become more pronounced. At ∼10 mol % DMSO molecules begin to penetrate into the bilayer, and the characteristic minimum in the density profile in the middle of the membrane is lost. At DMSO concentrations equal to or greater than 12.5 mol % for DPPC or 15.0 mol % for DOPC, pores in the bilayer form spontaneously. (See Figures 3d, 4d, and 5c.) These pores are toroidal in shape and lined with phospholipid head groups. The pores are filled with a mixture of DMSO and water and are stable for hundreds of nanoseconds. If the concentration of DMSO is increased further, then the pores become unstable and the membrane loses its integrity after 100−200 ns. Whereas the structure of the bilayer is lost, the phospholipids still cluster tightly together, suggesting that the system might eventually evolve into a series of micelles or, due to the periodic boundary conditions, tubes of phospholipids. (See Figure 5d.)

As noted above, the effect of DMSO on the structure of a model membrane has been previously examined. The most detailed study to date is that of Gurtovenko and Anwar,[27] who

dx.doi.org/10.1021/jp3035538 | J. Phys. Chem. B 2012, 116, 11911−11923

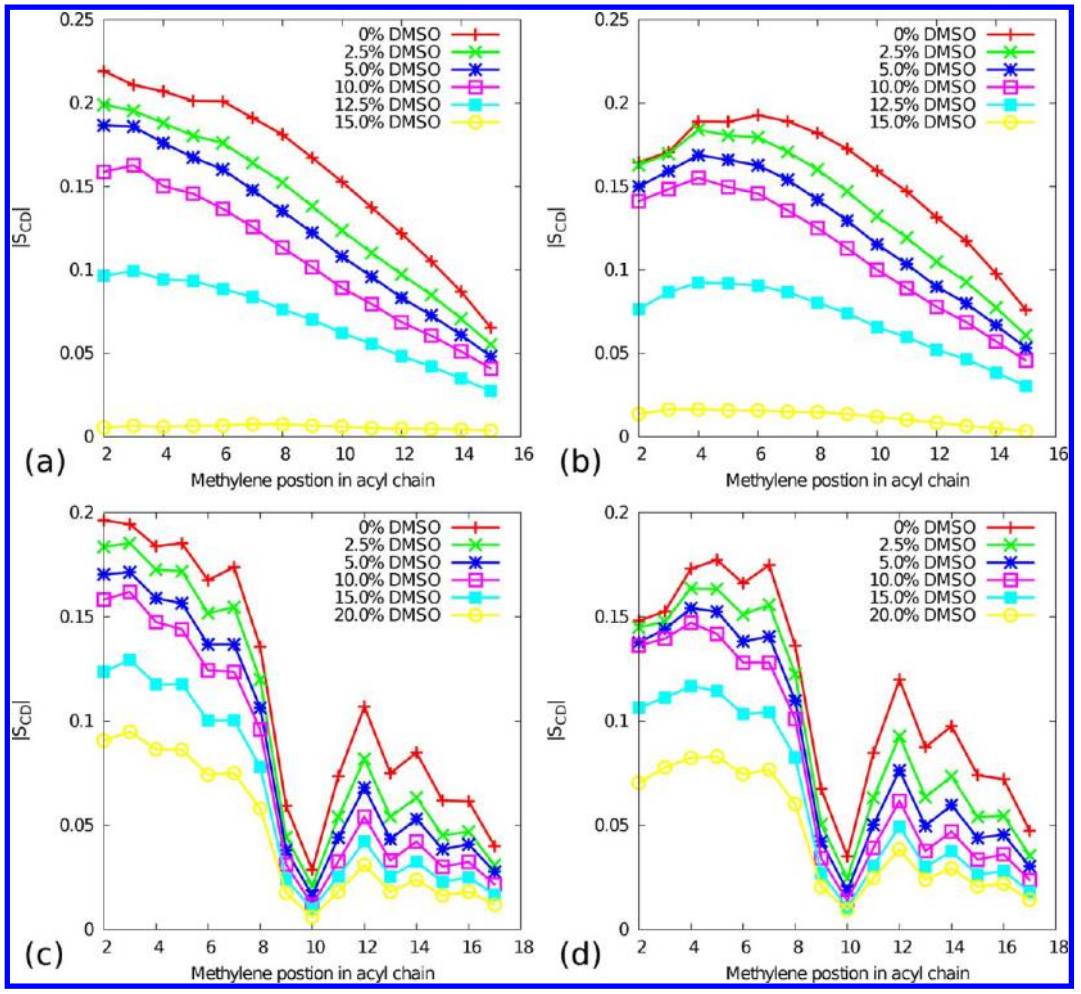

Figure 7. Order parameters of (a) the *sn*-1 chain of DPPC, (b) the *sn*-2 chain of DPPC, (c) the *sn*-1 chain of DOPC, and (d) the *sn*-2 chain of DOPC at different DMSO concentrations.

simulated a DPPC membrane in the presence of DMSO at concentrations ranging from 0 to 100 mol % for between 30 to 50 ns. In general, the results presented here are consistent with those of Gurtovenko and Anwar. At low concentrations (2.5−7.5 mol %) of DMSO the membrane thins, at intermediate concentrations (10.0−20.0 mol %) the formation of pores is observed, and at high concentrations of DMSO (25.0 mol %) the membrane is destroyed. However, there are some differences in the results, something that would be expected as different force fields were used. In their simulations, Gurtovenko and Anwar used the parameters developed by Berger et al.[49] for DPPC and Bordat et al.[50] for DMSO. The Berger parameters give rise to a DPPC bilayer that is less tightly packed than the G53A6$_L$ parameters, and thus the APL of a DPPC bilayer in water at 350 K is 0.690 and 0.654 nm^2 with the Berger and G53A6$_L$ force fields, respectively. The differences between the two DMSO models are relatively minor. In the G54A7 model, slightly higher charges are assigned to the sulfur and oxygen atoms than in the Bordat model. These differences in the force fields lead to differences in how DMSO is distributed in the membrane, especially at low DMSO concentrations. In this work, the peak in the DMSO density profile is at, or just above, the position of the phosphate headgroups, whereas in the simulations of Gurtovenko and Anwar the DMSO density peak is just below the phosphate headgroups. This highlights the fact that the effect of DMSO on membrane bilayers is due to the balance its hydrophobic and hydrophilic nature.[51−53] DMSO is sufficiently hydrophilic to be fully miscible with water and sufficiently hydrophobic to be able to cross membranes relatively easily. Another difference between the current study and previous work is the stability of the transmembrane pores. The concentration of DMSO required for the formation of pores within a bilayer, and their stability, will depend on a number of factors, with the force-fields used, the time-scales simulated, and the absolute number of solvent molecules per lipid being just a few of the factors that must be considered. In the initial work of Gurtovenko and Anwar[27] (with 29 solvent molecules per lipid), transmembrane pores formed spontaneously at DMSO concentrations of 10.0 mol % and above, whereas the membrane was no longer stable at 25.0 mol %. In a later study by the same group,[31] the number of solvent molecules per lipid was increased to 55. This caused the formation of pores to be observed at a concentration of only 7.0 mol % DMSO. In the current work, a concentration of 12.5 mol % was required to initiate pore formation, and increasing the number of solvent molecules per lipid did not appear to cause pores to form at a lower concentration. The differences between the results will in part be because the DMSO model used by Gurtovenko and Anwar is slightly less hydrophilic than that used in this work, and the bilayer itself is more stable when using the more recent GROMOS 54A7 parameters. Differences are also expected due to the time scales

dx.doi.org/10.1021/jp3035538 | J. Phys. Chem. B 2012, 116, 11911−11923

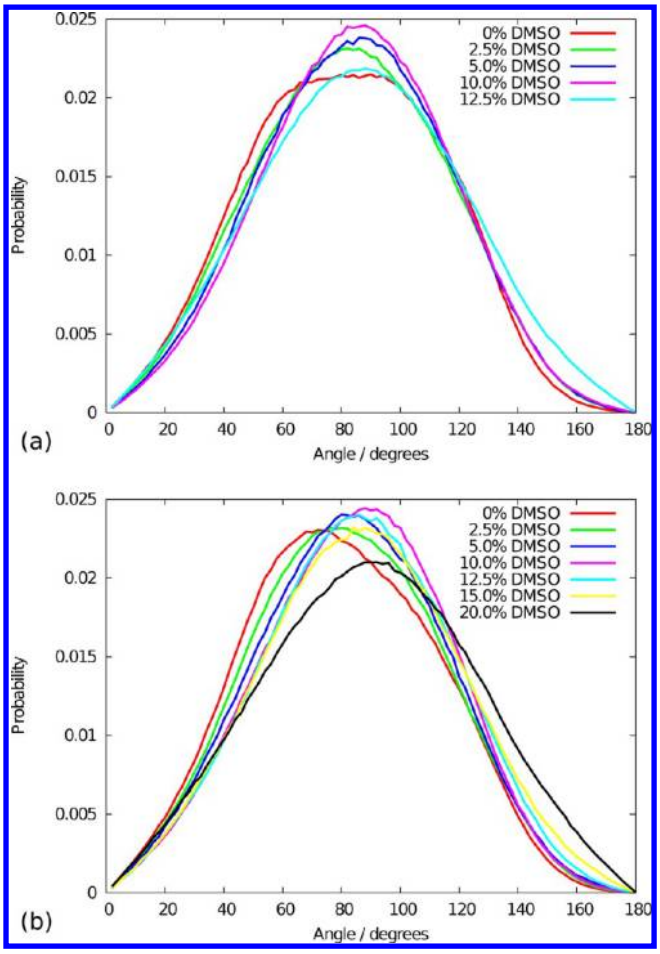

Figure 8. Probability distribution function of the angle between the bilayer normal, directed away from the middle of the bilayer, and the vector between the $P^{-}\rightarrow N^{+}$ atoms in the lipid headgroup for simulations of (a) DPPC and (b) DOPC in solutions of different DMSO concentration.

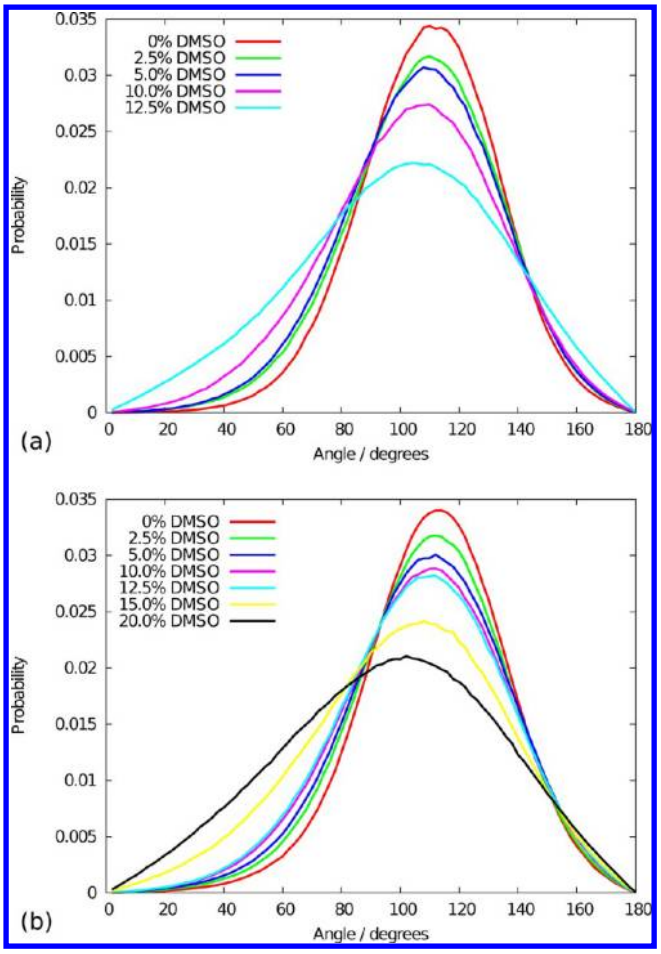

Figure 9. Probability distribution function of the angle between the bilayer normal, directed away from the middle of the bilayer, and the vector between the $O^{\delta-}\rightarrow C^{\delta+}$ atoms in the *sn*-1 carbonyl chain of the lipid for simulations of (a) DPPC and (b) DOPC in solutions of different DMSO concentration.

simulated. Most of the systems simulated by Gurtvenko and Anwar were simulated for 50 ns, whereas a few systems were simulated for longer. The DPPC membranes in this study would have appeared to be stable in DMSO concentrations up to 25.0 mol % if the time simulated had been limited to 100 or even 150 ns. The number of solvent molecules per lipid may be a factor in determining the threshold concentration required for pore formation. Below a certain point, increasing the number of solvent molecules per lipid will increase the number of DMSO molecules that will interact with the phospholipids, reducing the concentration at which a transmembrane pore forms. Ultimately, however, the lipids will be interacting with the maximum number of DMSO molecules that they are able to, and at this point increasing the number of solvent molecules per lipid further will not encourage the formation of pores. For the simulations performed in the current work, 46 solvent molecules per lipid is above this limit, as no pore was observed to form in a DPPC system at 10.0 mol % and 68 solvent molecules per lipid. (Indeed, as previously mentioned, the results of the two systems were, within statistical variation, the same.)

The effect of DMSO on a DOPC bilayer is broadly the same as that on a DPPC bilayer. The greatest difference appears to be in the stability of the different membranes in the presence of increasing amounts of DMSO and the point at which pore formation occurs. Not only is a higher concentration of DMSO needed to induce pore formation in a DOPC bilayer as compared with a DPPC bilayer but also once a pore has formed the membrane remains stable over a wider range of DMSO concentrations. One method of determining the greater resistance of DOPC to DMSO is through the calculation of the free energy barrier for the diffusion of DMSO across the membrane. As at even the lowest DMSO concentrations DMSO molecules are seen to pass through the membrane bilayers relatively frequently, the free energy profile could be readily calculated from the probability distribution using

$$\Delta G(z) = k_B T \ln(\rho_{eq}/\rho(z)) \quad (1)$$

where $\Delta G(z)$ is the change in free energy as a function of position along the direction normal to the bilayer, ρ_{eq} is the density of DMSO molecules in the bulk solution, and $\rho(z)$ is the density of DMSO along the direction normal to the bilayer. The free energy profiles calculated from eq 1 are shown in Figure 6 for both the DPPC and the DOPC membranes. (Plots were calculated using the last 60 ns of the simulations; only the concentrations of DMSO at which the membrane remained stable are shown.) As one would expect, the energy barriers for diffusion across the bilayers were reduced as the DMSO concentration increased, especially after the formation of a transmembrane pore. Figure 6 also clearly shows that the free

dx.doi.org/10.1021/jp3035538 | J. Phys. Chem. B 2012, 116, 11911−11923

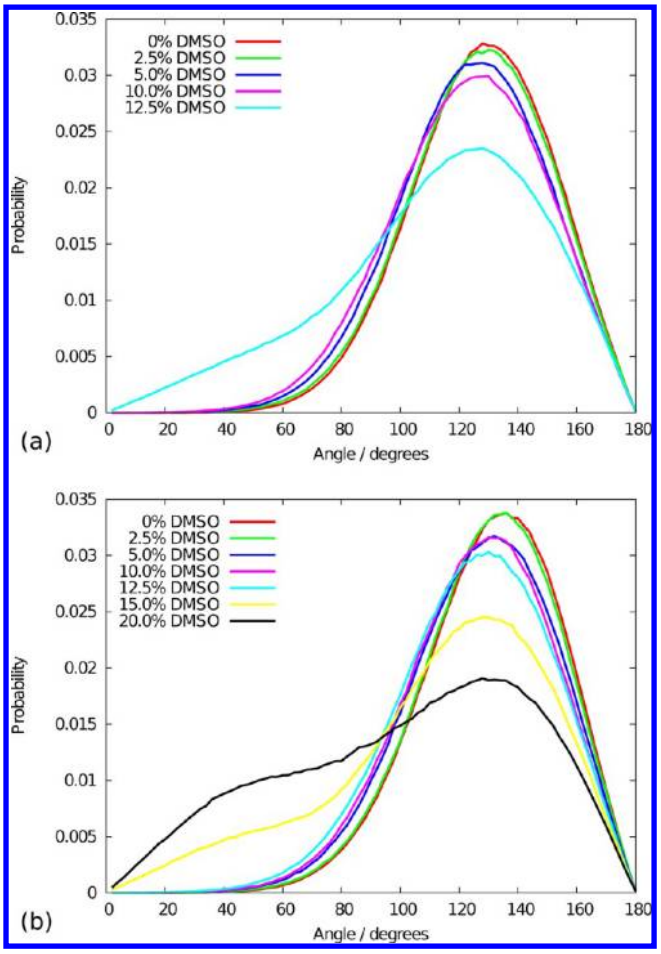

Figure 10. Probability distribution function of the angle between the bilayer normal, directed away from the middle of the bilayer, and the vector between the $O^{\delta-}\rightarrow C^{\delta+}$ atoms in the *sn*-2 carbonyl chain of the lipid for simulations of (a) DPPC and (b) DOPC in solutions of different DMSO concentration.

energy required for a DMSO molecule to diffuse across a membrane is higher in the case of a DOPC bilayer than for a DPPC bilayer. The longer acyl tail of the DOPC both stabilizes the membrane to DMSO (due to the greater dispersion forces present) and makes diffusion across the membrane by DMSO molecules more difficult.

The degree of ordering of the acyl chains of the phospholipids can be determined from the deuterium order parameter, S_{CD}, which provides a measure of the relative orientation of C−D bonds with respect to the bilayer normal. The order parameter can be calculated from

$$S_{CD} = \frac{1}{2}\langle 3\cos^2\theta - 1\rangle \quad (2)$$

where θ is the angle between a C−D of a methylene in the chain and the bilayer normal. Because the force field used in this work is a united-atom one, the positions of the deuteriums are derived from the positions of the neighboring carbons and assuming tetrahedral geometry of the methylenes. The calculated order parameters for both the *sn*-1 and *sn*-2 chains of the DPPC and DOPC lipids are shown in Figure 7. The presence of an unsaturated bond in the acyl chains of DOPC means that the lipid tails in DOPC are less well-ordered than those of DPPC, especially at the position of the carbon−carbon double bond (carbons 9 and 10). The interaction of DMSO with the membrane causes the acyl chains to become progressively more disordered as the concentration of DMSO increases. As with the membrane thickness, the order parameters decrease markedly at the point when pores form in the bilayer.

To determine in greater detail how the DMSO molecules interact with the headgroups of the phospholipids, we have calculated the probability distributions of the tilt angle between the bilayer normal, directed away from the center of the membrane, and the vectors between atoms associated with a number of important dipoles in the lipids. Tilt angles have been calculated for the $P^-\rightarrow N^+$ dipole moment, ζ_{PN}, and the *sn*-1 and *sn*-2 $O^{\delta-}\rightarrow C^{\delta+}$ carbonyl dipoles, ω_1 and ω_2, and are shown in Figures 8−10, respectively. The changes in ζ_{PN} caused by the presence of DMSO differ for the two phospholipid species. In the case of DPPC in aqueous solution, the $P^-\rightarrow N^+$ dipole moment tends to lie parallel to the plane of the bilayer. This behavior is unchanged at low DMSO concentrations, and whereas the angle distribution becomes more narrow, the peak of the distribution remains at ∼90°. In contrast, for the headgroups of DOPC, lipids in water are tilted slightly out of the plane of the bilayer. In the presence of DMSO there is a significant shift in ζ_{PN} to higher angles as the DMSO causes the lipid headgroups to tend to align themselves in manner similar to DPPC, with the $P^-\rightarrow N^+$ dipole moment parallel to the plane of the bilayer. The distributions of ω_1 and ω_2 behave in a similar manner for both lipids, the probability of the mode tilt angle being reduced as the DMSO concentration increases. For the *sn*-1 chain both lipids show a small shift to lower angles. Above the concentration required for pore formation the distribution changes noticeably, with low and high tilt angles becoming much more probable. The formation of pores is seen even more clearly in the distribution of ω_2, with a sharp increase in the probability of angles less than 80° being observed for both phospholipid species. These large changes in the angle distribution are caused by both the fact that some lipids rearrange themselves such that they form the sides of the pore, and are thus aligned parallel to the plane of the bilayer, and the fact that the membrane itself has become more undulated.

The radial distribution functions, $g(r)$, of the nitrogen atom (N) present in the lipid headgroup with the water oxygen (Ow), the DMSO oxygen (O), and the DMSO sulfur atom (S) are shown in Figure 11 for DOPC at four different concentrations. The equivalent radial distribution functions for DPPC are essentially identical (not shown). It is clear that whereas the height of each of the peaks is dependent on the concentration of DMSO, the position of the peaks in the case of $g_{NO}(r)$ and $g_{NS}(r)$ are essentially unchanged and show only a very minor shift in the case of $g_{NOw}(r)$. It is also clear that the DMSO oxygen atom can approach more closely to the nitrogen atom than either the water oxygen or the DMSO sulfur atom. The differences in the height of the peaks reflect a combination of changes in local packing as well as simply the normalization of the curves with respect to the average density of DMSO and water in the simulation box. A recent study[54] investigated the solvation structure of DMSO/water solutions around 1,2-dipropionyl-*sn*-glycero-3-phosphocholine using both neutron diffraction measurements combined with empirical potential structure refinement (EPSR) simulations and MD simulations. This study investigated only a single concentration, 30 mol %, at 300 K, but there is good agreement between the results of that study and those described in this article. Table 2 gives the

dx.doi.org/10.1021/jp3035538 | J. Phys. Chem. B 2012, 116, 11911−11923

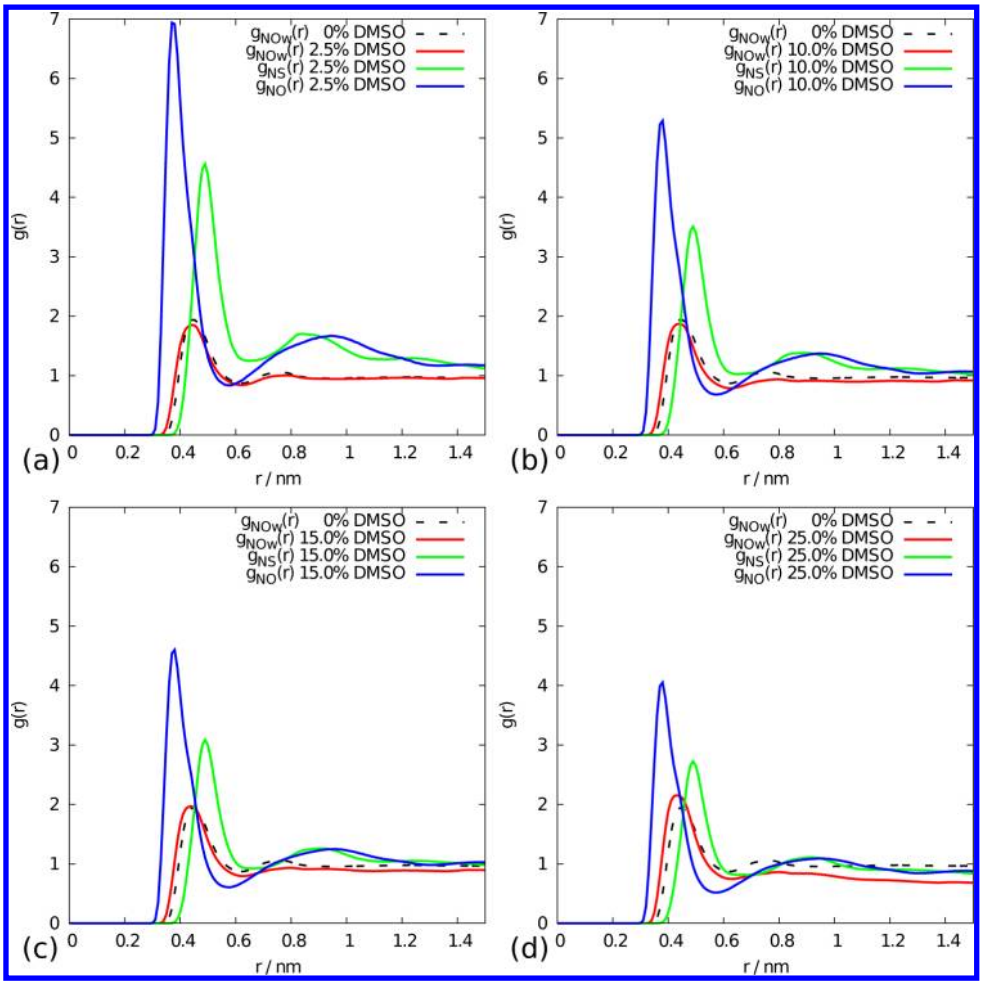

Figure 11. Radial distribution functions of the nitrogen (N) atom of DOPC with the water oxygen (Ow), the DMSO oxygen (O), and the DMSO sulfur (S) atoms at DMSO concentrations of (a) 2.5, (b) 10.0, (c) 15.0, and (d) 25.0 mol %. Also shown is the radial distribution function of the nitrogen atom of DOPC with the water oxygen atom in water.

Table 2. Number of Water Molecules in the First Solvation Shell of the Nitrogen Atom of the Phospholipid Headgroups for DPPC and DOPC at Different DMSO Concentrations

	coordination number	
DMSO concentration/mol %	DPPC	DOPC
0	15.9 ± 0.5	16.2 ± 0.5
1.25	15.2 ± 0.3	15.5 ± 0.4
2.50	14.8 ± 0.4	15.0 ± 0.5
5.00	13.6 ± 0.5	13.9 ± 0.4
10.0	12.2 ± 0.4	12.3 ± 0.6
12.5	11.7 ± 0.4	11.7 ± 0.5
15.0	10.4 ± 0.5	11.3 ± 0.5
20.0	9.5 ± 0.5	10.4 ± 0.4
25.0	9.4 ± 0.5	9.2 ± 0.5

number of water molecules in the first solvation shell around the nitrogen atom of DPPC and DOPC. As the concentration of DMSO increases the number of water molecules present in the first solvation shell of the nitrogen atom decreases, indicating that the choline group of the lipid is being dehydrated. Below 12.5 mol % DMSO, the coordination numbers of DPPC and DOPC are the same. At a concentration of DMSO at which the DPPC bilayers is no longer stable, the choline group of DOPC appears more hydrated than that of DPPC. After 25.0 mol % DMSO is reached and the DOPC bilayer has also lost its integrity, the values are again similar. Thus, the loss of the bilayer structures is accompanied by a dehydration of the choline group in excess of that due to the increased DMSO concentration alone.

Double-Bilayer Systems. Whereas the study of a single-bilayer system can provide useful information on how DMSO might interact with a cell membrane under equilibrium conditions, in reality cells will be exposed to a DMSO concentration gradient. Therefore, a set of simulations were performed on systems consisting of two bilayers and two separate solvent layers One layer initially contained an aqueous DMSO solution (layer A) and the other contained pure water (layer B). The overall concentrations of DMSO in the systems where 1.25 and 5.00 mol %.

Over the course of the simulations the diffusion of DMSO molecules through the bilayers was observed. On the time scales simulated (700−800 ns), only one of the systems fully equilibrated: the DPPC system at 1.25 mol %. The APL for this equilibrated double-bilayer system was measured to be 0.690 ± 0.007 nm^2 compared with 0.688 ± 0.011 nm^2 for the single-bilayer system. Indeed, all parameters measured for the equilibrated double-bilayer system were, within statistical variation, the same as those for the equivalent single-bilayer system. (See the Supporting Information for full details.) Figure 12 shows the how the concentration of each chamber changes over

dx.doi.org/10.1021/jp3035538 | J. Phys. Chem. B 2012, 116, 11911−11923

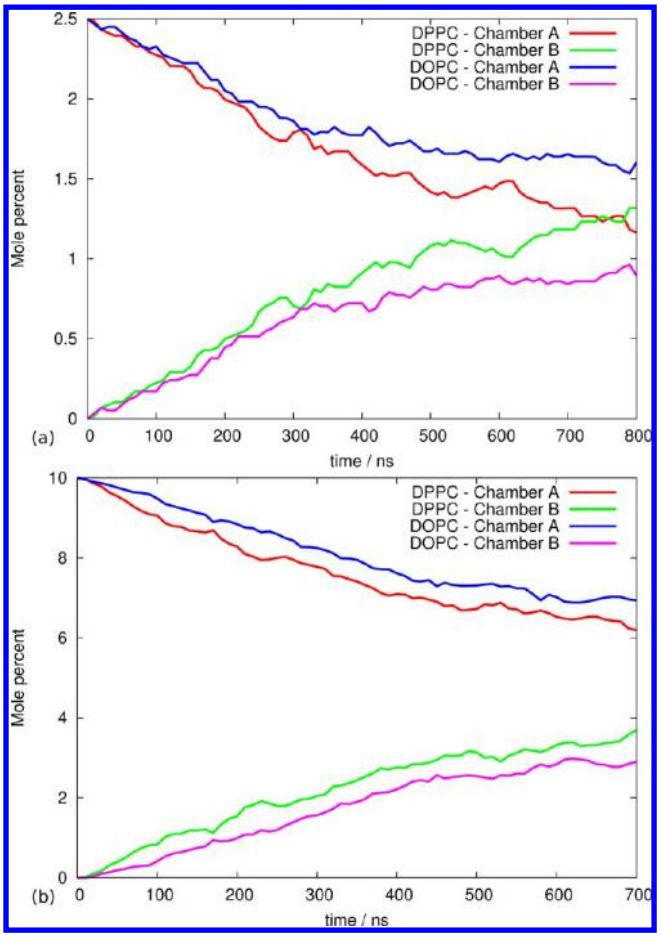

Figure 12. Concentration of the different chambers of the double-bilayer systems over the course of the simulations for (a) the 1.25 mol % systems and (b) the 5.00 mol % systems.

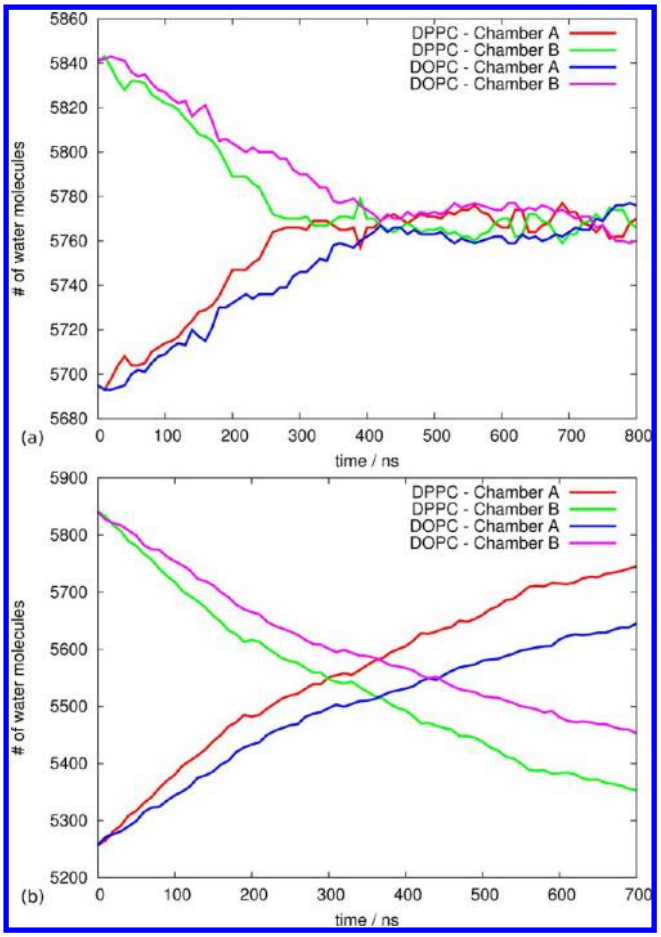

Figure 13. Number of water molecules in the different chambers of the double-bilayer systems over the course of the simulations for (a) the 1.25 mol % systems and (b) the 5.00 mol % systems.

the course of the simulations. It is clear that the DOPC bilayers equilibrate at a slower rate than the DPPC bilayers. Whereas the overall flow of DMSO molecules is from chamber A to chamber B, a few DMSO molecules are observed to flow in the opposite direction, that is, against the concentration gradient, as the simulation time increases. Accompanying the diffusion of DMSO molecules, there is also a flow of water molecules from chamber B to chamber A, as shown in Figure 13. As in the case of DMSO, the rate of flow is higher for DPPC than DOPC. At 1.25 mol % the number of water molecules in the two chambers is approximately equal after 300−400 ns and remains so for the remainder of the simulation. For the systems at 5.00 mol %, the number of water molecules in the two chambers has also equalized after 300−400 ns, but afterward the number of water molecules in chamber A continues to increase. These results illustrate how DMSO is able to dehydrate cells.

The simulation of the double-bilayer systems allows the investigation of the kinetics of the diffusion of DMSO molecules across the bilayers. Figure 14 shows the trajectories along the direction normal to the membrane bilayer of a few DMSO molecules during the first 20 ns of the simulation. The DMSO molecules selected are examples of those that pass from chamber A (high DMSO concentration) through the DPPC membranes to chamber B (low DMSO concentration). The data for the DOPC systems (not shown) are equivalent, indicating that the manner by which DMSO diffuses through the membranes is the same. In the systems where the concentration gradient was low (Figure 14a), the mechanism by which the DMSO molecules diffuse through the phospholipids involves three stages. The first stage involves the diffusion of the DMSO molecule from the bulk solution to a position below that of the phosphate groups of the lipids in the outer leaflet. This is a rapid process (taking only picoseconds) with DMSO molecules observed to jump back and forth across the headgroup. Once a molecule has diffused past the phosphate group it may remain situated in the area just below the headgroup for nanoseconds. The next stage involves the diffusion of the DMSO molecule from one side of the membrane to the other through the hydrophobic acyl chains. This process is again rapid, taking less than a nanosecond. The final stage of the process is the opposite of the first stage, involving a transition from a position below the phosphate groups of the inner leaflets into the bulk solution. These results agree with the mechanism proposed by Leekumjorn and Sum,[26] based on simulations of a system of two DPPC bilayers with an initial DMSO concentration gradient of 1.21 mol %. They also found that the diffusion of DMSO molecules across the membrane was a three-stage process.

At a DMSO concentration to 5.00 mol %, the individual stages become less well-defined and the diffusion process tends to merge into a single one (Figure 14b). The position between the phosphate headgroups and the acyl chains becomes less stable, with the DMSO molecules spending more time in the region of the lipid tails and the diffusion of a molecule from one

dx.doi.org/10.1021/jp3035538 | J. Phys. Chem. B 2012, 116, 11911−11923

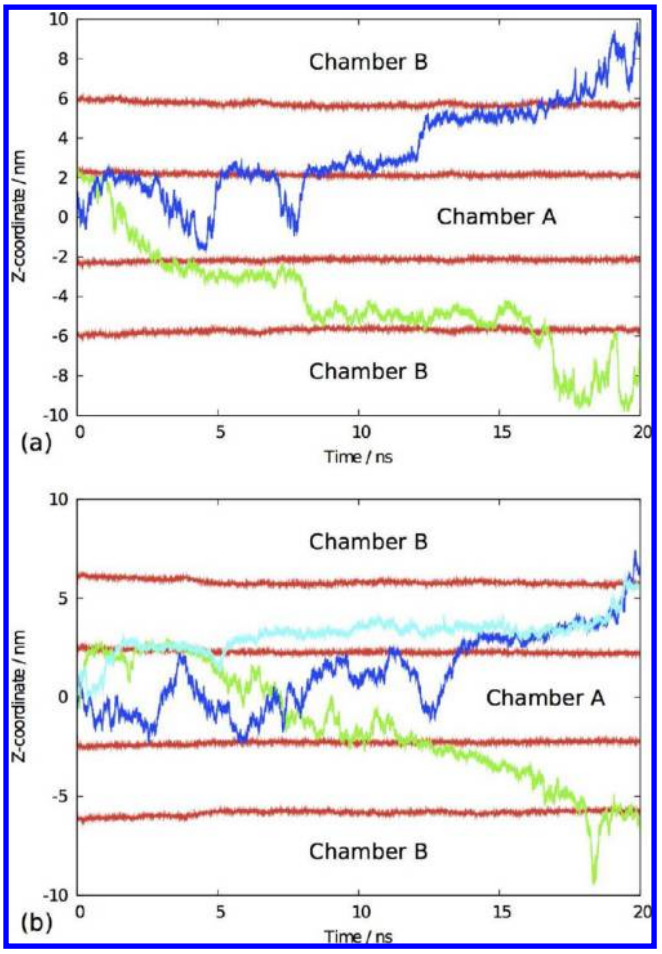

Figure 14. Trajectories along the z axis (normal to the bilayers) of DMSO molecules that diffuse through the DPPC membrane (shown by the blue and green lines). Taken from the first 20 ns simulation of a system with a DMSO concentration of (a) 1.25 and (b) 5.00 mol % at 350 K. The red lines indicate the positions of the phosphate groups.

side of the membrane to the other being far more gradual. The increased concentration of DMSO within the membrane is consistent with the free energy profiles shown in Figure 6. At low concentrations, there is a free energy well ~2 nm from the center of the membrane, right above the position of the phosphate groups. Just above this free energy minimum there is a weak local minimum, corresponding to the position right below the lipid headgroups, followed by a sharp peak in the free energy due to the hydrophobic lipid tails. As the concentration of DMSO in solution is increased the height of the barrier is reduced and the peak broadens.

As previously mentioned, Leekumjorn and Sum[26] studied a DPPC double-bilayer system with an initial DMSO concentration gradient of 1.21 mol % (95 DMSO molecules in 7584 water molecules). After 95 ns, they found that 9 DMSO molecules had diffused through the bilayers. They used data determined from the simulation to calculate the rate of diffusion according to Fick's law. Fick's Law of diffusion states that

$$\frac{dn}{dt} = \frac{AK_pD}{z_M}(C_B - C_A) \tag{3}$$

where n is the number of DMSO molecules in the initial solution, t is the time, K_p is the partition coefficient of DMSO for the lipid and aqueous phases at equilibrium, D is the diffusion coefficient of DMSO through the bilayer, A is the area of the membrane normal to the plane of the bilayer, and z_M is the thickness of the membrane. If A is constant, then the above equation can be rewritten as

$$\frac{dn}{dt} = \frac{K_pD}{z_M}\left(\frac{n_0 - n}{z_B} - \frac{n}{z_A}\right) \tag{4}$$

where n_0 is the initial number of DMSO molecules in chamber A and z_A and z_B is the thickness of chambers A and B, respectively. The partition coefficient, K_p, of DMSO between the lipid and aqueous regions is given by

$$K_p = \frac{C_{lipid}}{C_{aqueous}} = \frac{N_{lipid}/z_{lipid}}{N_{aqueous}/z_{aqueous}} \tag{5}$$

where C is the concentration of DMSO, N is the number of DMSO molecules in, and z is the thickness of the lipid and aqueous phases, respectively, at equilibrium. Using eq 4, Leekumjorn and Sum predicted that it would take 2000 ns for the system to equilibrate fully and found that the simulation results differed from the model by about 13% at 95 ns.

The parameters z_A, z_B, z_M, and D have been determined from each double-bilayer system and are given in Table 3. The thickness of the various regions was calculated using the average center of mass position of the phosphate groups as the boundary points. The diffusion coefficients were taken from the average of 25 molecules, but despite this the range of values was quite wide, resulting in a relatively large error. The diffusion coefficients in Table 3 are slightly larger than those calculated by Leekumjorn and Sum ($3.74 \pm 1.00 \times 10^{-6}$ cm^2 s^{-1}) but agree well. Because the double-bilayer simulations did not reach equilibrium, the partition coefficients were calculated from the results of the single-bilayer simulations at the same concentration, using the method outlined by Leekumjorn and Sum.[26] DMSO molecules were determined to be in the lipid region if they were below the average center of mass position of the third carbons in the acyl tails. DMSO molecules not in the lipid region were determined in be in the aqueous region if they were not within the first solvation shell (0.72 nm) of a phosphorus atom. Those DMSO molecules closer than 0.72 nm to a phosphorus atom were determined to be in the interfacial region and were therefore were not counted. The partition coefficients determined form the results of this study are much larger than that calculated (0.088) in the previous study.

Figure 15 shows the rate of diffusion predicted using Fick's Law compared against the simulation results for the different

Table 3. Parameters Required for the Calculation of the Rate of Diffusion of DMSO Using Fick's Law

	parameter				
lipid (total DMSO concentration/mol %)	K_p	D	z_A	z_B	z_M
DPPC (1.25)	0.496	0.472 ± 0.297	4.31 ± 0.99	4.16 ± 0.99	3.35 ± 0.99
DPPC (5.00)	0.351	0.461 ± 0.241	4.84 ± 0.99	4.14 ± 0.99	3.32 ± 0.99
DOPC (1.25)	0.351	0.594 ± 0.119	4.29 ± 0.99	4.23 ± 0.99	3.63 ± 0.99
DOPC (5.00)	0.280	0.495 ± 0.204	4.59 ± 0.99	4.02 ± 0.99	3.50 ± 0.99

dx.doi.org/10.1021/jp3035538 | J. Phys. Chem. B 2012, 116, 11911−11923

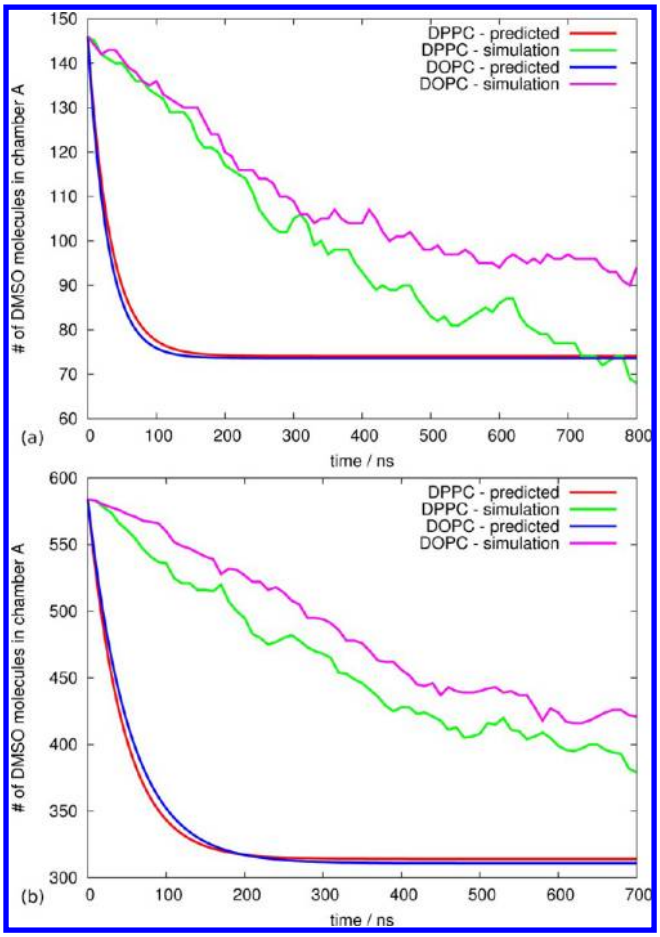

Figure 15. Number of water molecules in chamber A of the double-bilayer systems over the course of the simulations compared against the number predicted from Fick's Law for (a) the 1.25 mol % systems and (b) the 5.00 mol % systems.

systems. It is clear that the systems appear to take significantly longer to equilibrate than is predicted from Fick's Law. Part of the difference between the two may be due the error associated with the parameters used to calculate the rate of diffusion, especially the rate of diffusion and the partition coefficient. Another source of error will arise from the fact that the APL has been assumed to be constant over the course of the simulation, but in actual fact the APL does drift over the course of the simulations, especially for the systems at 5.00 mol % DMSO. The thicknesses of the various regions (chamber A, chamber B, and the membranes) are also not constant over the course of the simulation. Whereas the comparison between the rate of diffusion predicted by Fick's Law and those observed in the simulations is useful, it is important to remember that Fick's Law is only applicable for bulk behavior, not atomistic. For example, according to Fick's Law, the number of DMSO molecules in chamber A should never increase. However, in MD simulations molecules will occasionally diffuse against the concentration gradient and temporary increase the number of DMSO molecules in the high concentration region, as we have observed.

CONCLUSIONS

MD simulations of DPPC and DOPC bilayers in aqueous/DMSO solutions of varying concentration have been used to investigate the effect of DMSO on the stability of lipid bilayers. The results suggest that increasing concentrations of DMSO result in the progressive thinning of the membrane, followed by pore formation and ultimately loss of the membrane integrity. Whereas these general observations are in line with previous studies, this work has highlighted the importance of considering an extended time scale. In some cases the bilayers remained metastable for hundreds of nanoseconds before either a pore formed spontaneously or, at high DMSO concentrations, the structure of the bilayer was lost completely.

The effect of DMSO on DOPC bilayers was found to be broadly the same as that on DPPC bilayers. In both cases, the APL increasing and the membrane become thinner with increasing DMSO concentration. Beyond a given threshold concentration pores formed spontaneously in the membrane. The DOPC bilayers were, however, more resistant to the effects of DMSO than the DPPC bilayers. This is most likely due to the increased length of the lipid tails in DOPC. In addition, the free energy barrier associated with the diffusion of a DMSO molecule across the bilayer was higher for DOPC than DPPC.

In addition to investigating the effects of DMSO on single-bilayer systems, a series of double-bilayer systems with a concentration gradient have also been simulated. These simulations showed that both DMSO and water molecules diffuse across the bilayers in an attempt to equalize the concentration. The mode of diffusion of DMSO molecules across the membrane bilayer is dependent on the concentration of DMSO. At low concentrations, a DMSO molecule diffuses through phospholipid bilayers in three stages with a clearly defined minimum in the free energy profile just below the lipid headgroups. At higher concentrations these local minima are no longer evident, and diffusion across the membrane occurs in a single transition. The rate of diffusion determined from simulation was compared against that predicted by Fick's Law, and it was found that the time needed f or the systems to equilibrate was longer than predicted. This discrepancy is partially due to the errors in the calculation of Fick's Law but also reflects the fact that Fick's Law starts to break down at the atomistic level.

Determining the effects of DMSO on model membranes provides valuable information that can be used to assist in the understanding of molecular level events during the pre- and post-cryopreservation process. By determining the action of DMSO on membranes of different composition and structure, it is possible for simulations to help assist in the development of better cryosolvent solutions. The work discussed above, determining how changing the phospholipid present in the membrane alters the behavior of the membrane, represents the first step in this process. Future work will investigate the action of DMSO on more realistic membranes containing a mixture of different species.

ASSOCIATED CONTENT

Supporting Information

The coordinate files of equilibrated bilayers of DPPC at 0, 2.5, 5.0, 10.0, and 12.5 mol % and DOPC at 0, 2.5, 5.0, 10.0, 12.5, and 15.0 mol % are provided. This information is available on the GROMOS Automated Topology Builder and Repository (http://compbio.chemistry.uq.edu.au/atb).[47] In addition, data showing the equivalence of the single and double DPPC bilayers systems at 1.25 mol % DMSO are provided. This material is available free of charge via the Internet at http://pubs.acs.org.

AUTHOR INFORMATION

Corresponding Author

*E-mail: R.Mancera@curtin.edu.au.

Notes

The authors declare no competing financial interest.

■ ACKNOWLEDGMENTS

This research was supported by Australian Research Council (ARC) Linkage Grant LP0884027 with further financial support from Alcoa of Australia and BHP Billiton Worsley Alumina. The computational resources were provided by iVEC. We thank E. Bunn, A. Kaczmarczyk, and B. Funnekotter at the Botanic Gardens and Parks Authority (BGPA) in WA for valuable discussions.

■ REFERENCES

(1) Meryman, H. T.; Williams, R. J.; Douglas, M. S. J. *Cryobiology* **1977**, *14*, 287−302.
(2) Wusteman, M.; Robinson, M.; Pegg, D. *Cryobiology* **2004**, *48*, 179−189.
(3) Engelmann, F. *In Vitro Cell. Dev. Biol.* **2004**, *40*, 427−433.
(4) Day, J. G.; Harding, K. C.; Nadarajan, J.; Benson, E. E. *Mol. Biomethods Handb.* **2008**, 917−947.
(5) Kaczmarczyk, A.; Rokka, V.-M.; Keller, E. R. J. *Potato Res.* **2011**, *54*, 45−79.
(6) Kaczmarczyk, A.; Turner, S. R.; Bunn, E.; Mancera, R. L.; Dixon, K. W. *In Vitro Cell. Dev. Biol.* **2011**, *47*, 17−25.
(7) Benson, E. E.; Harding, K.; Johnston, J. W. *Methods Mol. Biol.* **2007**, *368*, 163−183.
(8) Sakai, A.; Engelmann, F. *CryoLetters* **2007**, *28*, 151−172.
(9) Benson, E. E. *Crit. Rev. Plant Sci.* **2008**, *27*, 141−219.
(10) Lovelock, J. E.; Bishop, M. W. H. *Nature* **1959**, *183*, 1394−1395.
(11) Anchordoguy, T. J.; Carpenter, J. F.; Crowe, J. H.; Crowe, L. M. *Biochim. Biophys. Acta* **1992**, *1104*, 117−122.
(12) Mandumpal, J. B.; Kreck, C. A.; Mancera, R. L. *Phys. Chem. Chem. Phys.* **2011**, *13*, 3839−3842.
(13) Kreck, C. A.; Mandumpal, J. B.; Mancera, R. L. *Chem. Phys. Lett.* **2011**, *501*, 273−277.
(14) Menon, A.; Funnekotter, B.; Kaczmarczyk, A.; Bunn, E.; Turner, S. R.; Mancer, R. L. *CryoLetters* **2012**, *33*, 259−270.
(15) Colucci, M.; Maione, F.; Bonito, M. C.; Piscopo, A.; Giannuario, A. D.; Pieretti, S. *Pharmacol. Res.* **2008**, *57*, 419−425.
(16) Haigler, H. J.; Spring, D. D. *Ann. N. Y. Acad. Sci.* **1983**, *411*, 19−27.
(17) Ahkong, Q. F.; Fisher, D.; Tampion, W.; Lucy, J. A. *Nature* **1975**, *253*, 194−195.
(18) Gordeliy, V. I.; Kiselev, M. A.; Lesieur, P.; Pole, A. V.; Teixeira, J. *Biophys. J.* **1998**, *75*, 2343−2351.
(19) Kiselev, M. A.; Lesieur, P.; Kisselev, A. M.; Grabielle-Madelmond, C.; Ollivon, M. *J. Alloys Compd.* **1999**, *286*, 195−202.
(20) Shashkov, S. N.; Kiselev, M. A.; Tioutiounnikov, S. N.; Kiselev, A. M.; Lesieur, P. *Physica B* **1999**, *271*, 184−191.
(21) Yamashita, Y.; Kinoshita, K.; Yamazaki, M. *Biochim. Biophys. Acta, Biomembr.* **2000**, *1467*, 395−405.
(22) Yu, Z. W.; Quinn, P. J. *Biochim. Biophys. Acta, Biomembr.* **2000**, *1509*, 440−450.
(23) Spindler, R.; Wolkers, W. F.; Glasmacher, B. *CryoLetters* **2011**, *32*, 148−157.
(24) Smondyrev, A. M.; Berkowitz, M. L. *Biophys. J.* **1999**, *76*, 2472−2478.
(25) Sum, A. K.; de Pablo, J. J. *Biophys. J.* **2003**, *85*, 3636−3645.
(26) Leekumjorn, S.; Sum, A. K. *Biochim. Biophys. Acta, Biomembr.* **2006**, *1758*, 1751−1758.
(27) Gurtovenko, A. A.; Anwar, J. *J. Phys. Chem. B* **2007**, *111*, 10453−10460.
(28) Huang, C. H.; Lapides, J. R.; Levin, I. W. *J. Am. Chem. Soc.* **1982**, *104*, 5926−5930.
(29) Notman, R.; Noro, M.; O'Malley, B.; Anwar, J. *J. Am. Chem. Soc.* **2006**, *128*, 13982−13983.
(30) Gurtovenko, A. A.; Anwar, J. *J. Phys. Chem. B* **2007**, *111*, 13379−13382.
(31) Gurtovenko, A. A.; Onike, O. I.; Anwar, J. *Langmuir* **2008**, *24*, 9656−9660.
(32) Gurtovenko, A. A.; Anwar, J.; Vattulainen, I. *Chem. Rev.* **2010**, *110*, 6077−6103.
(33) Moldovan, D.; Pinisetty, D.; Devireddy, R. V. *Appl. Phys. Lett.* **2007**, *91*, 204104.
(34) Lin, J.; Novak, B.; Moldovan, D. *J. Phys. Chem. B* **2012**, *116*, 1299−1308.
(35) Funnekotter, B.; Kaczmarczyk, A.; Turner, S. R.; Bunn, E.; Zhou, W.; Smith, S.; Flematti, G.; Mancera, R. L., Submitted to *Cryobiology*.
(36) Poger, D.; van Gunsteren, W. F.; Mark, A. E. *J. Comput. Chem.* **2010**, *31*, 1117−1125.
(37) Poger, D.; Mark, A. E. *J. Chem. Theory. Comput.* **2010**, *6*, 325−336.
(38) Lewis, R. N. A. H.; Sykes, B. D.; McElhaney, R. N. *Biochemistry* **1988**, *27*, 880−887.
(39) Schmid, N.; Eichenberger, A. P.; Choutko, A.; Riniker, S.; Winger, M.; Mark, A. E.; van Gunsteren, W. F. *Eur. Biophys. J.* **2011**, *40*, 843−856.
(40) Berendsen, H. J. C.; Postma, J. P. M.; van Gunsteren, W. F.; Hermans, J. In *Intermolecular Forces*; Reidel: Dordrecht, The Netherlands, 1981.
(41) Oostenbrink, C.; Villa, A.; Mark, A. E.; van Gunsteren, W. F. *J. Comput. Chem.* **2004**, *25*, 1656−1676.
(42) van der Spoel, D.; Lindahl, E.; Hess, B.; Groenhof, G.; Mark, A. E.; Berendsen, H. J. C. *J. Comput. Chem.* **2005**, *26*, 1701−1718.
(43) Patra, M.; Hyvonen, M. T.; Falck, E.; Sabouri-Ghomi, M.; Vattulainen, I.; Karttunen, M. *Comput. Phys. Commun.* **2007**, *176*, 14−22.
(44) Karttunen, M.; Rottler, J.; Vattulainen, I.; Sagui, C. In *Computational Modeling Of Membrane Bilayers*; Feller, S., Ed.; Elsevier Academic Press: San Diego, CA, 2008; Vol. *60*, pp 49−89.
(45) Allen, M. P.; Tildesley, D. J. *Computer Simulation of Liquids*; Oxford University Press: New York, 1989.
(46) Berendsen, H. J. C.; Postma, J. P. M.; van Gunsteren, W. F.; Dinola, A.; Haak, J. R. *J. Chem. Phys.* **1984**, *81*, 3684−3690.
(47) Malde, A. K.; Zuo, L.; Breeze, M.; Stroet, M.; Poger, D.; Nair, P. C.; Oostenbrink, C.; Mark, A. E. *J. Chem. Theory Comput.* **2011**, *7*, 4026−4037.
(48) Leekumjorn, S.; Sum, A. K. *Biophys. J.* **2006**, *90*, 3951−3965.
(49) Berger, O.; Edholm, O.; Jahnig, F. *Biophys. J.* **1997**, *72*, 2002−2013.
(50) Bordat, P.; Sacristan, J.; Reith, D.; Girard, S.; Glattli, A.; Muller-Plathe, F. *Chem. Phys. Lett.* **2003**, *374*, 201−205.
(51) Mancera, R. L.; Chalaris, M.; Samios, J. *J. Mol. Liq.* **2004**, *110*, 147−153.
(52) Mancera, R. L.; Chalaris, M.; Refson, K.; Samios, J. *Phys. Chem. Chem. Phys.* **2004**, *6*, 94−102.
(53) Mancera, R. L.; Chalaris, M.; Samios, J. In *Recent Advances in the Understanding of Hydrophobic and Hydrophilic Effects: A Theoretical and Computer Simulation*; Kluwer Academic Publishers: Boston, 2004; pp 987−396.
(54) Dabkowska, A. P.; Foglia, F.; Lawrence, M. J.; Lorenz, C. D.; McLain, S. E. *J. Chem. Phys.* **2011**, *135*, 225105.